J. Nanosci. Tech. - Volume 3 Issue 2 (2017) 256–259

Share Your Innovations through JACS Directory

Journal of Nanoscience and Technology

Visit Journal at http://www.jacsdirectory.com/jnst

ISSN: 2455-0191

Development of GO-ZrO_2 Nanocomposite: Enhanced Photocatalytic Degradation of Cr(VI) under Sunlight Irradiation

B. Prashanti, T. Damodharam*

Department of Environmental Sciences, Sri Venkateswara University, Tirupati – 517 502, Andhra Pradesh, India.

ARTICLE DETAILS

Article history:
Received 11 September 2017
Accepted 21 September 2017
Available online 06 October 2017

Keywords:
Graphene-ZrO_2
FE-SEM
Photocatalytic Degradation

ABSTRACT

The photocatalytic degradation of hexavalent chromium using GO-ZrO_2 nanocomposite, the GO- ZrO_2 nanocomposite was prepared by hydrothermal method and prepared GO-ZrO_2 nanocomposite was characterized by X-ray diffractometer (XRD), field emission scanning electron microscope (FE-SEM) with energy dispersive absorption X-ray spectroscopy (EDAX), transmission electron microscope (TEM), UV-Vis spectrophotometer, respectively. The results show that in the nanocomposite the ZrO_2 nanoparticles were densely coated on the GO nanosheets, which display a good combination between graphene and ZrO_2 nanoparticles. The GO-ZrO_2 nanocomposite exhibits an enhanced photocatalytic performance in the reduction of Cr(VI) with removal rate 98% under UV light irradiation.

1. Introduction

Nowadays, the rapid change in environment affected by pollution is a key factor contributing to the global warming. Among the various types of the environmental pollution, water pollution is the most important. Water is majorly polluted by a various chemicals around the world owing to the rapid industrialization and urbanization [1]. The heavy metals are well known water pollutants, which are highly toxic and carcinogenetic and resistant to direct degradation or reduction by day-light driven and are consequently classified as importunate pollutants [2]. Chromium is a widespread pollutant in the environment which commonly originates from the wastewater produced from tanning, electroplating, water cooling and other industries [3]. The release and subsequent accumulation of these toxic compounds in aquatic media create extreme risk to the environment. Chromium have two most common oxidation states. Cr(VI) is more toxic than Cr(III) because it is carcinogenic and mutagenic to living organisms[4,5]. The department of health and human services (DHHS) and U.S. environmental protection agency (EPA) have identified Cr(VI) as a carcinogenic element and allowed limiting concentration as<100 mg/L in drinking water[6]. Therefore, the removal of Cr(VI) is imperative to meet the discharge levels. The most current efficient and economical method to remove heavy metals by photocatalytic degradation using day-light driven in the presence of an appropriate photocatalyst that is able to promote the reduction of toxic metals to favorable byproducts.

Among the carbon materials, graphene has become a rising star due to its unique two-dimensional (2D) structure, high electron conductivity and mobility, and high surface area [7-9]. Especially, graphene- based semiconductor composite photocatalysts have been extensively applied to photocatalytic degradation of organic compounds, solar cells, water splitting to hydrogen and selective organic transformations [7, 8, 10-19]. In fact, graphene based metal oxides nanocomposites have also attracted research attention in recent years. For example Madadrang et al., [20] introduced the high adsorption behavior of EDTA-GO nanocomposite for the removal of Pb(II) in aqueous solution. Zhao et al., [21] reported that highly dispersed sulfonated graphene nanosheets showed very high adsorption capacities for the removal of naphthalene and 1-naphthol from aqueous solutions. Wen et al., [22] have been reported the LDH/Go nanocomposites showed much higher adsorption capacity and excellent ability to removal of As(V) from aqueous solutions. Li et al., [23] have been prepared that GO/Fe_3O_4 nanosheets can be used that as an sorbent for the simple and rapid removal of Cu(II) from aqueous solution. Thakur et al., [24] reported that sulfur/reduced graphene oxide nanohybrid for effective removal of mercury ions from water at around pH 6-8. Fan et al., [25] have been reported the synthesis of graphene oxide decorated with magnetic cyclo dextrin for fast chromium removal. Zhu et al., [26] have reported the one-pot synthesis of magnetic graphene nanocomposites decorated with core @ double-shell nanoparticles for fast chromium removal. The development of nanomaterials has acquired great significance in recent years due to their high efficiency and fast rates on water treatment. However, the study of graphene based nanocomposites for waste water treatment is still in the early stage.

In this present work, we have reported a hydrothermal method for the synthesis of high-efficiency graphene-based zirconiumoxide (GO-ZrO_2) nanocomposites with short time, high adsorption capacity for the removal of chromium(VI) from aqueous water.

2. Experimental Methods

2.1 Synthesis of Graphite Oxide

Graphite oxide was synthesized from graphite, using a modified hummer's method [27]. In a typical procedure, about 5 g of graphite powder was added to 115 mL of concentrated (98%) H_2SO_4 in an ice bath with stirring for 30 min. A 15 g of $KMnO_4$ was added slowly to the above mixture with stirring and cooling for 30 min. Subsequently, 2.5 g of $NaNO_3$ was added with continuous stirring for 1 hr. So that the temperature of the mixture maintained below 15 °C during that time. The temperature of mixture then raised to 40 °C with water bath, and the mixture was continuously stirred for 30 min. After that, the mixture was diluted by 800~1000 mL of distilled water, the temperature of which then raised to 98 °C. The mixture was then added by H_2O_2 (30%) until gas evolution ceased followed by filtering. The color of the dispersion turned from black to yellow. The product was washed repeatedly with 1 M HCl (5%) and distilled water until the pH value of the product arrived at near 7. Then the product was dried in an air oven at 60 °C to obtain graphite oxide.

2.2 Synthesis of GO-ZrO_2 Nanocomposite

To synthesis GO-ZrO_2 composite, synthesized graphite oxide (20 mg) dissolved in 20 ml distilled water and sonication for 1 hr to get suspension GO. And then mixed zirconium nitrate was dissolved in distilled water and zirconium hydroxide was precipitated by drop wise addition of sodium hydroxide (maintaining constant pH about 11) with stirring. The mixture was transferred autoclave for hydrothermal treatment at 170 °C for 24 hrs.

*Corresponding Author
Email Address: thotidamodharam@yahoo.co.in (T. Damodharam)

Cite this Article as: B. Prashanti, T. Damodharam, Development of GO-ZrO_2 nanocomposite: enhanced photocatalytic degradation of Cr(VI) under sunlight irradiation, J. Nanosci. Tech. 3(2) (2017) 256–259.

The final resulting mixture was washed with distilled water then dried at 80 °C for overnight in hot air oven. The synthesis procedure was shown in below (Fig. 1).

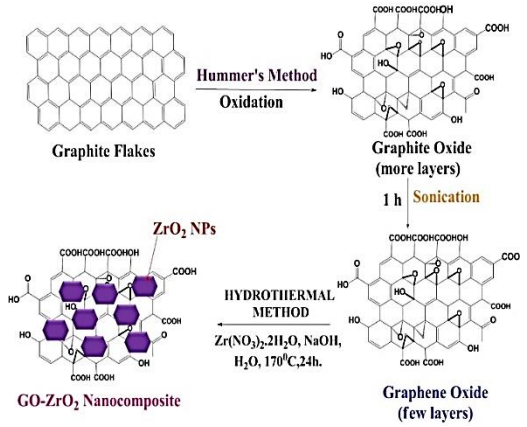

Fig. 1 Illustration of chemical route synthesis of GO-ZrO_2 nanocomposite

2.3 Characterization of Photocatalysts

The structure and morphology of the samples were characterized by X-ray diffractometry (XRD) Bruker D8 using CuKα1 (1.5406 Å) and Kα2 (1.54439 Å) radiations, scanning electron microscope (SEM) imaging with energy dispersive spectroscopy (EDS) using a carl zeiss model ultra 55 microscope operating at 5 and 20 kV, and transmission electron microscope (TEM) measurements were performed on a Tecnai G^2FEI F12 I at 200 kV. Raman spectra were recorded using a WiTec alpha 200 SNOM system. Nitrogen adsorption and desorption experiments were carried out on micromeritics ASAP 2020 analyzer. The samples were out gassed at 150 °C for 12 hr in a dynamic vacuum before physisorption measurements. The specific surface area was calculated using Brunauere Emmette Teller (BET) method. A photoluminescence spectrum (PL) was recorded by using Jobinyvon Flurolog-3 spectrofluorometer with YSOW Xenon lamp as used broad band source. Shimadzu-1800 UV-visible Spectrometer to determine the concentration of heavy metal ions. pH of the solution was calculated by Elico pH meter.

2.4 Photocatalytic Activity Studies

The photodegradation tests of heavy metal Cr(VI) ions were performed using the GO, ZrO_2, GO-ZrO_2 and mechanical mixture of GO and ZrO_2 solids according to the following procedure: The photocatalyst powder (0.03 g) was dispersed in a 100 mL sealed glass beaker containing 30 mL of Cr(VI) solution with concentration of 0.014 g/L in glass beaker. The mixture was sonicated for 5 min and stirred for 30 min in the dark in order to reach adsorption-desorption equilibrium. At the given time intervals a sample of 3 mL was taken from the mixture and immediately centrifuged to remove the dispersed photocatalysts. The concentration of the clean transparent solution was analyzed by checking the absorbance at 400 nm for Cr(VI) with the UV-vis spectrophotometer, which denoted as C_t. The reproducibility was checked by repeating the measurements atleast three times and was found to be within the acceptable limit (± 5%).

3. Results and Discussion

The synthesized graphite oxide and GO-ZrO_2 were first characterized with XRD. As displayed in (Fig. 2b), the pattern of graphite oxide has a typical characteristic peak centered at 2 theta = 9.92°. The most intense peak for graphite at 2 Theta = 26.37° is absent in the GO sample, confirming the high quality of graphite oxide. In the pattern of graphite oxide, the reappearance of the diffraction line at 24.37° and disappearance of the diffraction peak at 9.92° give evidence that the graphite oxide was restored the ordered crystal structure. From (Fig. 2c) gives the XRD patterns of as-synthesized GO-ZrO_2. The dominant peaks located at ca. 24.06°, 24.45°, 28.18°, 31.47° and 51.20° are indexed to (011), (110), (111), (111) and (221) crystallographic planes of monoclinic ZrO_2 consistent with GO-ZrO_2 composite. Through search and contrast via the JADE 5.0 database, it was found that the XRD pattern matched the standard XRD pattern (JCPDS No. 83-0937), the corresponding diffraction is indexed in (Fig. 2c), and no characteristic peaks of impurities are observed, suggesting pure ZrO_2 was prepared [28]. Notably, no typical diffraction peaks of the GO are observed in the GO-ZrO_2. The reason can be attributed to the fact that the low amount and the relatively low diffraction intensity of GO.

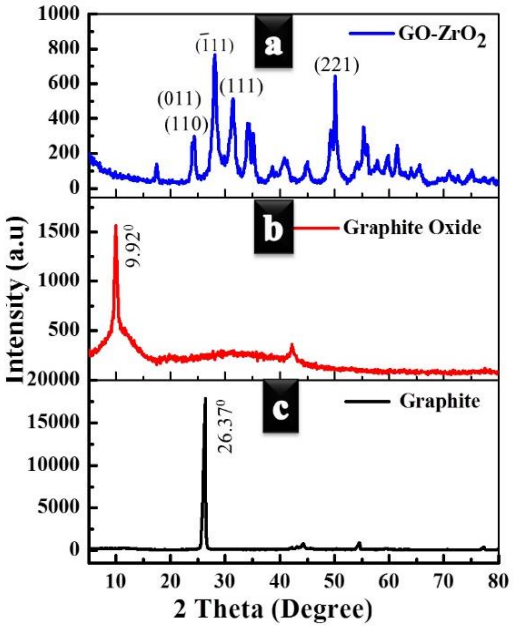

Fig. 2 XRD pattern of the (a) GO-ZrO2, (b) graphite oxide and (b) graphite.

Raman spectroscopy is a powerful and widely used technique for characterizing the sp^2 and sp^3 hybridized carbon atoms contained in graphene oxide to identify disorder and defect structures. Generally in GO based samples, the disorder-induced D bands arise from the tangential stretch and sp^3-hybridized carbon and the G band represents the crystalline graphite with E_{2g} zone center mode; moreover, the I_D/I_G ratio depends strongly on the amount of disorder in the graphitic material. The I_D/I_G ratio should increase when more defects are introduced into GO. According to (Fig. 3), the I_D/I_G ratio of GO-ZrO_2 composite is 0.992 which is higher than the 0.970 calculated from GO. That is to say, ZrO_2 modification can be effective in bringing an amount of defects into the structure of GO [29].

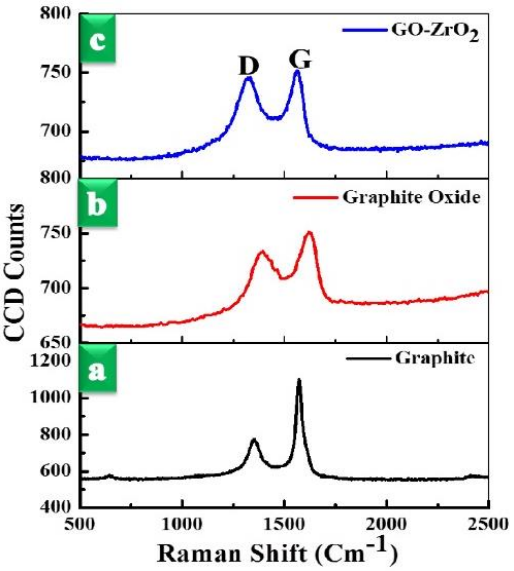

Fig. 3 Raman Spectra of (a) Graphite, (b) Graphite Oxide, and GO-ZnO_2

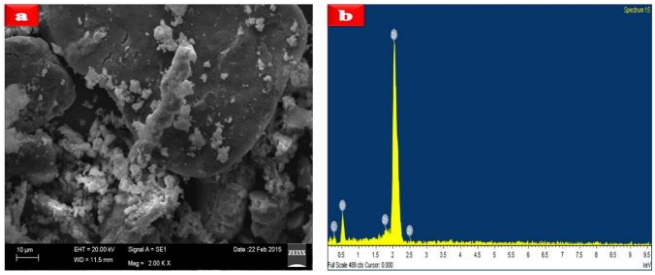

Fig. 4 (a) SEM image and (b) EDS spectrum of GO-ZrO_2

The SEM of nanocomposite was taken as powder synthesized, images were taken on carbon tape. From the (Fig. 4a) shows the SEM images. It is unambiguous that the morphology of intercalated nanocomposite particles are really in nanosize and it shows the clumsy morphology due to the aggregation of particles in the solution while synthesis. From (Fig. 4b) shows the energy dispersive spectrum (EDS) results of the GO-ZrO_2 nanocomposite. Zr, O and C elements are observed.

From (Fig. 5) illustrates the typical TEM images of GO-ZrO_2 nanocomposite. It can be clearly seen that the exfoliated GO sheet was decorated by hexagonal shape of ZrO_2, with size range between 10-75 nm. From (Fig. 5d) displays selective area electron diffraction (SAED) pattern of hybrid material shows the fusion of super lattices which are characteristic nature of the layer structure of any kind of materials.

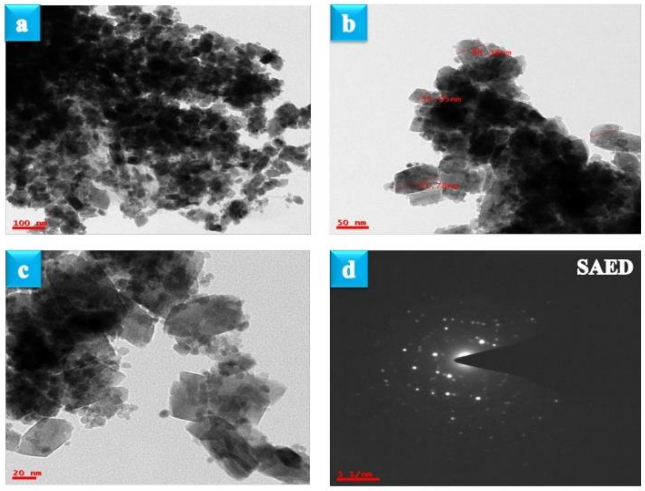

Fig. 5 (a), (b), (c) TEM images and (d) SEAD pattern of GO-ZrO_2.

HR-TEM images of the GO-ZrO_2 fusion material show springes in 5 nm range we observed this kind of springes only in the case of material is crystalline nature. From the P-XRD we observed the crystalline nature of the hybrid material as well as graphene oxide this is confirmed by HR-TEM. In HR-TEM we observed springes on ZrO_2 shows hexagonal form (Fig. 6).

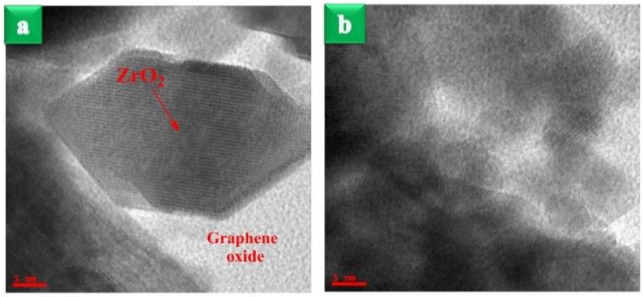

Fig. 6 HRTEM images of GO-ZrO_2.

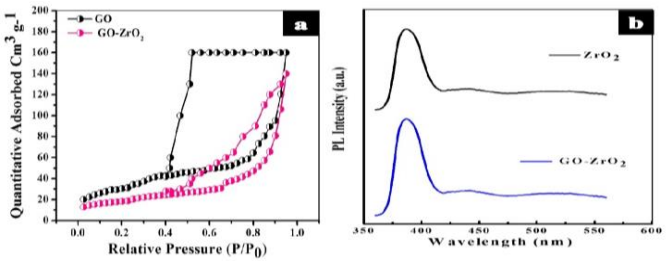

Fig. 7 (a) Nitrogen adsorption-desorption isotherms and (b) photoluminescence spectra of ZrO2 and GO-ZrO2 composite.

We have carried out the Brunauer-Emmett-Teller (BET) analysis to understand the specific surface area of the as prepared GO and GO-ZrO_2 composites and the corresponding nitrogen adsorption-desorption isotherm curves are shown in (Fig. 7a). Surface area of GO-ZrO_2 (207.1 m^2g^{-1}) was higher than that of GO (186 m^2g^{-1}) due to the high density of ZrO_2 hexagonal shaped nanocrystals. The high surface area of GO-ZrO_2 suggests enhanced photocatalytic activity of inorganic pollutants degradation. From (Fig. 7b) shows the emission spectra of ZrO_2 and GO-ZrO_2 samples, respectively. The samples show a strong broad-band emission ranging from 350 to 600 nm centered at 388 nm. The emission peak and strength depends upon the species and densities of PL. High crystal quality and quantum confinement in the nanostructures are two factors favoring the increase of the intensity of light emission at room temperature. Also, the observed PL emission peak of ZrO_2 at 388 nm is in good agreement with that of ZrO_2 nanoparticles at 387 nm [30].

3.1 Photocatalytic Activity of GO-ZrO_2

From (Figs. 8a and b) shows the change in the UV-Vis absorbance spectra of Cr(VI) solution with different irradiation intervals over the GO-ZrO_2 samples. As mentioned in the experimental section, the catalyst was equilibrated with the Cr(VI) ions to check for adsorption of the heavy metal on the solid photocatalyst. The UV-Vis absorption spectra of Cr(VI) have a characteristic peak at 398 nm. The UV-Vis results indicate that Cr(VI)was degraded during the reaction. The decrease in the absorbance of the solution was due to the destruction of the homo and hetero-polyaromatic rings present in the Cr(VI) ions.

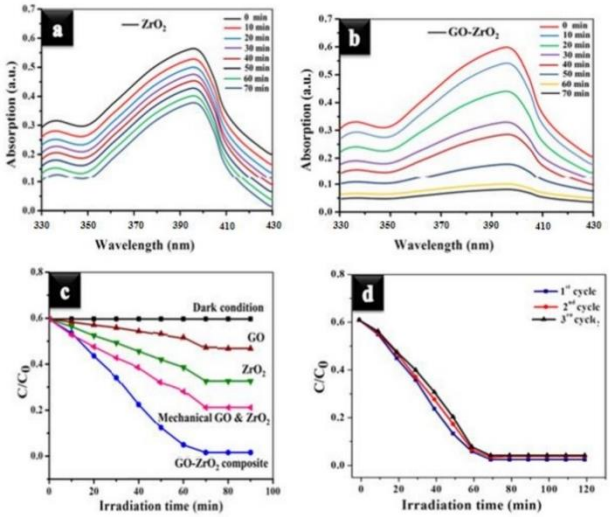

Fig. 8 The progress of UV-Vis spectra for Cr(VI) solution with (a) ZrO_2 (b) GO-ZrO_2 (c) comparision study of Photocatalytic activity (d) three cycles of GO-ZrO_2 in photodegradition of Cr(VI).

The photocatalytic activity of the GO-ZrO_2 samples was determined by monitoring the degradation of the Cr(VI) ions. A blank experiment was carried out to confirm that the photodegradation reaction did not proceed without the presence of catalyst. The photocatalytic degradation of Cr(VI) in aqueous solution under the solar light irradiation was carried out at regular time intervals was shown in Fig. 8c. The absorption of these solutions decreased gradually with irradiation time. The characteristic absorption of Cr(VI)almost disappeared after about 70 min, and the color of Cr(VI) solution changed gradually from yellow blue to colorless after irradiation for 70 min. At concentration 0.014 g/L of Cr(VI) ions degradation was 98%, which shows the GO-ZrO_2 Ncs was excellent photocatalyst**.** The ZrO_2 shows the degradation of Cr(VI) removal is 45%, graphite oxide removal is 22% and mechanical mixing of GO+ZrO_2 is 62%. The GO-ZrO_2 composite material possesses much higher photocatalytic activity than pure ZrO_2, GO and mechanical mixture of GO+ZrO_2. The catalyst was found to be active for three cycles without any major deactivation, and more than 95% degradation was achieved in all experiments within 70 min using the GO-ZrO_2 catalyst. The reusability of the GO-ZrO_2 nanocomposite was ascribed to the low photo-corrosive effect and high catalytic stability of the synthesized GO-ZrO_2 sample.

Fig. 9 has explained the mechanism of high photocatalyticactivity for GO-ZrO_2. Under solar light, the photoelectron and hole are emitted. Then the photoelectron is transferred to GO to resist the recombination photoelectron and hole because it is energetically favorable. The transferred photoelectrons react with the absorbed O_2 on the surface of GO to form ·OH, which is used to degrade heavy metal Cr(VI) ion. Additionally, the remaining hole in ZrO_2 takes part in the redox reaction to generate ·OH, Owing to the high specific surface area and superior electron mobility of GO, an appropriate integration of GO and ZrO_2 would give rise to a hybrid nanocomposite to achieve high photodegradation activity [31]. In this case, the recombination of photo-generated electrons and holes is suppressed, and their lifetime is prolonged. GO hybridized ZrO_2 exhibited enhanced photocatalytic efficiency for the degradation of inorganic pollutants.

Cite this Article as: B. Prashanti, T. Damodharam, Development of GO-ZrO_2 nanocomposite: enhanced photocatalytic degradation of Cr(VI) under sunlight irradiation, J. Nanosci. Tech. 3(2) (2017) 256–259.

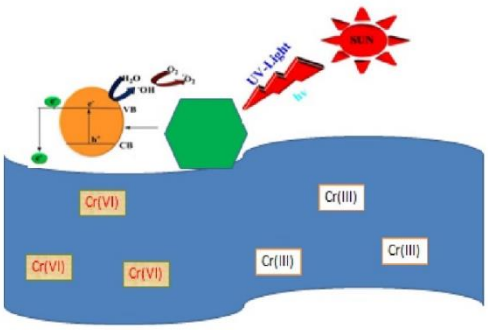

Fig. 9 Proposed mechanism of Cr(VI) removable by GO/ZrO_2 nanocomposite.

4. Conclusion

GO-ZrO_2 nanocomposite was successfully synthesized via hydrothermal. The experimental results indicate that (i) GO-ZrO_2 nanocomposite exhibit high-quality photocatalytic performance. (ii) The high photocatalytic performance is ascribed to the increased light absorption intensity and range as well as the reduction of photoelectron–hole pair recombination in ZrO_2 with the introduction of GO-ZrO_2 nanocomposite achieves a highest Cr(VI) removal rate of 98%. Our findings provide necessary information to understand the mechanism in enhanced photocatalytic property in GO-ZrO_2 system and to guide further research for effective and efficient photo catalysts. It is expected that GO-ZrO_2 can be applied as novel adsorbent for Cr(VI) removal from wastewater.

Acknowledgement

We gratefully acknowledge instrumental support University of Hyderabad.

References

[1] R.A. Goyer, Handbook on toxicity of inorganic compounds, Marcel Dekker, New York, 1988.
[2] S.H. Yu, H. Li, Q. Yao, S.Q. Fu, G.T. Zhou, Microwave-assisted preparation of sepiolite-supported magnetite nanoparticles and their ability to remove low concentrations of Cr(VI), RSC Adv. 5 (2015) 84471-84482.
[3] D. Park, Y.S. Yun, J.Y. Kim, J.M. Park, How to study Cr(VI) biosorption: Use of fermentation waste for detoxifying Cr(VI) in aqueous solution, Chem. Eng. J. 136 (2008) 173-179.
[4] P. Miretzky, A.F. Cirelli, Cr(VI) and Cr(III) removal from aqueous solution by raw and modified lignocellulosic materials: A Review, J. Hazard. Mater. 180 (2010) 1-19.
[5] Y. Lin, W. Cai, X. Tian, X. Liu, G. Wang, C. Liang, Polyacrylonitrile/ferrous chloride composite porous nanofibers and their strong Cr-removal performance, J. Mater. Chem. 21 (2011) 991-997.
[6] C.F. Gonzalez, D.F. Ackerley, C.H. Park, A. Matin, A soluble flavoprotein contributes to chromate reduction and tolerance by *Pseudomonas putida*, Acta Biotechnol. 23 (2003) 233-239.
[7] N. Zhang, Y. Zhang, Y.J. Xu, Recent progress on graphene-based photocatalysts: current status and future perspectives, Nanoscale 4 (2012) 5792-5813.
[8] Q. Xiang, J. Yu, M. Jaroniec, Graphene-based semiconductor photocatalysts, Chem. Soc. Rev. 41 (2012) 782-796.
[9] H.P. Cong, X.C. Ren, P. Wang, S.H. Yu, Macroscopic multifunctional graphene-based hydrogels and aerogels by a metal ion induced self-assembly process, ACS Nano. 6 (2012) 2693-2703.
[10] J. Chen, C. Li, G. Eda, Y. Zhang, W. Lei, M. Chhowalla, W.I. Milne, W.Q. Deng, Incorporation of graphene in quantum dot sensitized solar cells based on ZnO nanorods, Chem. Commun. 47 (2011) 6084-6086.
[11] N.R. Khalid, E. Ahmed, Z. Hong, M. Ahmad, Synthesis and photocatalytic properties of visible light responsive La/TiO_2-graphene composites, Appl. Surf. Sci. 263 (2012) 254-259.
[12] Q. Li, B. Guo, J. Yu, J. Ran, B. Zhang, H. Yan, J.R. Gong, Highly efficient visible-light-driven photocatalytic hydrogen production of CdS-cluster-decorated graphene nanosheets, J. Am. Chem. Soc. 133 (2011) 10878-10884.
[13] Z. Wang, B. Huang, Y. Dai, Y. Liu, X. Zhang, X. Qin, J. Wang, Z. Zheng, H. Cheng, Crystal facets controlled synthesis of graphene@TiO_2 nanocomposites by a one-pot hydrothermal process, Cryst. Eng. Comm. 14 (2012) 1687-1692.
[14] Q. Xiang, J. Yu, M. Jaroniec, Preparation and enhanced visible-light photocatalytic H_2-production activity of graphene/C_3N_4 composites, J. Phys. Chem. C 115 (2011) 7355-7363.
[15] Q. Xiang, J. Yu M. Jaroniec, Synergetic effect of MoS_2 and graphene as co-catalysts for enhanced photocatalytic H_2 production activity of TiO_2 Nanoparticles, J. Am. Chem. Soc. 134 (2012) 6575-6578.
[16] T. Xu, L. Zhang, H. Cheng Y. Zhu, Significantly enhanced photocatalytic performance of ZnO via graphene hybridization and the mechanism study, Appl. Catal. B. 101 (2011) 382-387.
[17] J. Zhang, J. Yu, M. Jaroniec, R. Gong, Noble metal-free reduced graphene oxide-$Zn_xCd_{1-x}S$ nanocomposite with enhanced solar photocatalytic H_2-production performance, Nano. Lett. 12 (2012) 4584-4589.
[18] X. Zhou, T. Shi, H. Zhou, Hydrothermal preparation of ZnO-reduced graphene oxide hybrid with high performance in photocatalytic degradation, Appl. Surf. Sci. 258 (2012) 6204-6211.
[19] Q. Xiang, J. Yu, M. Jaroniec, Enhanced photocatalytic H_2-production activity of graphene-modified titania nanosheets, Nanoscale 3 (2011) 3670-3678.
[20] C.J. Madadrang, H.Y. Kim, G. Gao, N. Wang, J. Zhu, H. Feng, M. Gorring, M.L. Kasner, S. How, Adsorption behavior of EDTA-graphene oxide for Pb (II) removal, ACS Appl. Mater. Interf. 4 (2012) 1186–1193.
[21] G.X. Zhao, L. Jiang, Y.D. He, J.X. Li, H.L. Dong, X.K. Wang, W.P. Hu, Sulfonated graphene for persistent aromatic pollutant management, Adv. Mater. 23 (2011) 3959-3963.
[22] T. Wen, X. Wu, X. Tan, X. Wang, A. Xu, One-Pot synthesis of water-swellable Mg–Al layered double hydroxides and graphene oxide nanocomposites for efficient removal of As(V) from aqueous solutions, ACS Appl. Mater. Interf. 5 (2013) 3304-3311.
[23] J. Li, S. Zhang, C. Chen, G. Zhao, X. Yang, J. Li, X. Wang, Removal of Cu(II) and fulvic acid by graphene oxide nanosheets decorated with Fe_3O_4 nanoparticles, ACS Appl. Mater. Interf. 4 (2012) 4991–5000.
[24] S. Thakur, G. Das, P.K. Raul, N. Karak, Green one-step approach to prepare sulfur/reduced graphene oxide nanohybrid for effective mercury ions removal, J. Phys. Chem. C 117 (2013) 7636–7642.
[25] L. Fan, C. Luo, M. Sun, H. Qiu, synthesis of graphene oxide decorated with magnetic cyclodextrin for fast chromium removal, J. Mater. Chem. 22 (2012) 24577-24583.
[26] J. Zhu, S. Wei, H. Gu, B.R. Sowjanya, Q. Wang, Z. Luo, N.H. David, P. Young, Z. Guo, One-post synthesis of magnetic graphene nanocomposites decorated with core @ double- shell nanoparticles for fast chromium removal, Environ. Sci. Technol. 46 (2012) 977-985.
[27] Y. Zhang, H. HuiJuan Chi, W.H. Zhang, Y. Sun, Q. Qing Liang, Y. Gu, R. Jing, Highly efficient adsorption of copper ions by a PVP-reduced graphene oxide based on a new adsorptions mechanism, Nano-Micro Lett. 6(1) (2014) 80-87.
[28] S. Rani, M. Kumar, S. Sharma, D. Kumar, S. Tyagi, Effect of graphene in enhancing the photo catalytic activity of zirconium oxide, Catal. Lett. 144 (2014) 301-307.
[29] H. Teymourian, A. Salimi, S. Frioozi, A. Korani, S. Soltanian, One-pot hydrothermal synthesis of zirconium dioxide nanoparticles decorated reduced graphene oxide composite as high performance electrochemical sensing and biosensing platform, Electrochem. Acta 143 (2014) 196-206.
[30] H. Cao, X. Qiu, B. Luo, Y. Liang, Y. Zhang, R. Tan, M. Zhao, Q. Zhu, Synthesis and room-temperature ultraviolet photoluminescence properties of zirconia nanowires, Adv. Funct. Mater. 14(3) (2014) 243-246.
[31] S. Giri, D. Ghosh, C. Kumar Das, Growth of vertically aligned tunable polyaniline on graphene/ZrO_2 nanocomposites for supercapacitor energy-storage application, Adv. Funct. Mater. 24 (2014) 1312-1324.